

# RSC Advances



This is an *Accepted Manuscript*, which has been through the Royal Society of Chemistry peer review process and has been accepted for publication.

*Accepted Manuscripts* are published online shortly after acceptance, before technical editing, formatting and proof reading. Using this free service, authors can make their results available to the community, in citable form, before we publish the edited article. This *Accepted Manuscript* will be replaced by the edited, formatted and paginated article as soon as this is available.

You can find more information about *Accepted Manuscripts* in the [Information for Authors](#).

Please note that technical editing may introduce minor changes to the text and/or graphics, which may alter content. The journal's standard [Terms & Conditions](#) and the [Ethical guidelines](#) still apply. In no event shall the Royal Society of Chemistry be held responsible for any errors or omissions in this *Accepted Manuscript* or any consequences arising from the use of any information it contains.

## ARTICLE

## Periodic indentation patterns fabricated on AlGaInP light emitting diodes and their effects on light extraction

Cite this: DOI: 10.1039/x0xx00000x

Received 00th January 2014,  
Accepted 00th January 2014

DOI: 10.1039/x0xx00000x

[www.rsc.org/](http://www.rsc.org/)

Xiaoyu Lin, Duo Liu<sup>a</sup>), Guanjun Lin, Qian Zhang, Naikun Gao, Dongfang Zhao, Ran Jia, Zhiyuan Zuo, Xiangang Xu

We report a novel method for fabricating periodic indentation patterns on AlGaInP light emitting diodes (LEDs) that can effectively improve the light extraction efficiency. The patterns consist of hemispherical pits created by direct imprinting the top GaP window layer of AlGaInP LEDs with patterned sapphire (PS). The angle resolved electroluminescent tests reveal that the patterned chips show an average light emission enhancement of 155% over the original planar chips.

### Introduction

The past decade has witnessed extensive applications of light emitting diodes (LEDs) as lighting sources for traffic signals, outdoor displays, liquid crystal display (LCD) back lighting, and recently, general lighting applications.<sup>1,2</sup> However, most commercial white LEDs still suffer from low efficacy and poor colour rendering properties due to inherent absence of red colour. As a result, red LEDs were proposed to be integrated into white LED units for warm white lighting with high colour rendering index (CRI) and high efficacy. Currently, high brightness red LEDs are mainly manufactured based on aluminium gallium indium phosphide (AlGaInP) alloy.<sup>3,4</sup> Varying the molar fraction of AlGaInP alloy enables direct band-gap emission of red, orange, yellow and green colors.<sup>5</sup> However, like their InGaN counterparts, AlGaInP LEDs also suffer from low light extraction efficiency (LEE) due to total internal reflection at the air/device interface and Urbach absorption.<sup>6-8</sup> The Shell's law indicates that the LEE ( $\eta$ ) of a planar LED is related to the reflective index  $n$  by  $\eta \approx 1/(4n^2)$ .<sup>9</sup> As AlGaInP has a very large refractive index ( $\sim 3.5$  at 630 nm), merely  $\sim 2.3\%$  of total electroluminescent photons can escape from the surface of a planar AlGaInP LED.<sup>6,7</sup>

Recently, a variety of techniques have been developed to improve the LEE of LEDs, including surface roughening,<sup>10-12</sup> surface patterning by using optical, e-beam or ion-beam lithography,<sup>13</sup> patterned substrate<sup>14</sup> and plasmonic nanostructures.<sup>15,16</sup> The essential design principle is to create additional optical channels for photons to escape from LED surface. Among these, photonic crystal (PC) LEDs have attracted much attention. 2D-PCs can significantly increase the LEE of a LED by 1) scattering guided modes into radiation

modes, and 2) inhibiting particular guided modes by photonic band gap. However, fabricating PCs on LEDs usually requires expensive and bulky facilities for precise control of electrons, lasers or ions,<sup>17-21</sup> which greatly hinders their applications.

Patterned sapphire substrates (PSSs) have been widely used for the growth of high brightness GaN-based blue LEDs. The adoption of PSSs has two technological advantages. First, they can reduce the density of threading dislocations by interrupting and/or bending them, thus increasing the internal quantum efficiency (IQE). Second, they can intercept the guided optical modes in LEDs and force them to escape from the chips; thus greatly increasing the LEE.<sup>9,22</sup>

In this paper, we report a new method that can effectively improve the LEE of AlGaInP LEDs by using patterned sapphire as arrayed indenters to create periodic hemispherical pits on the GaP window layer of AlGaInP LEDs. We achieved a 155% enhancement on the LEE and the formation mechanisms of the periodic pits were discussed based on the classical indentation theory.

### Experimental details

The AlGaInP LED wafers used in this study were grown on GaAs substrate by metal-organic chemical vapor deposition (MOCVD). The LED wafers contain, from bottom to top, a GaAs substrate, a distributed Bragg reflector, a 1  $\mu\text{m}$  n-AlGaInP, 20 pairs of GaInP/AlGaInP multiple quantum wells (MQWs), a 1  $\mu\text{m}$  p-AlGaInP, and an 8  $\mu\text{m}$  GaP:Mg window layer. The GaP window layer is oriented 15° off-axis from [100] to [111] with crystallographic (511) plane exposed. We selected patterned sapphire as arrayed indenter to fabricate patterns on LED wafers because of its superior hardness and

mechanical stability. The patterned sapphires were purchased from North Microelectronics Company (NMC, Beijing, China), which have periodically distributed hexagonal cones similar to Mongolian yurts, as shown in Fig. 1(a). The patterned sapphires and the LED wafers were first supersonorically cleaned by acetone, alcohol, and deionized water in sequence, each for 15 min, respectively. After drying, a wafer was placed face up onto a self-made stainless steel mould and then covered by a patterned sapphire. The sample was then pressed by a hydrostatic machine. Figure. 1(b-d) show a deionized water of the fabrication process. Periodic pits with desired indentation depth were created on the wafer after pressure and duration optimization. The wafer was carefully cleaned to remove possible contaminations, e.g. small fragments. The surface morphology of the sample was then examined by optical microscopy (Olympus BX51, Japan). Scanning electron microscopy (SEM, Hitachi S-4800, Japan) was carried out to study both the top view and the cross sectional features of the indented sample. The electrical and optical properties of the LEDs were examined by a source-measurement unit (Keithley 2400, USA), a fibre spectrometer (Avantes Spec-2048, Netherlands), and a probe station (Suss PM5, Germany). We have optimized the loading conditions of this method after more than 80 tests. It is found that it is necessary to avoid lateral friction during the indentation process. In rare cases, hydrostatic delay in the loading cycle could cause specimen smash, which can be avoided by reducing the loading rate. After parameter optimization, the reproducibility of this method can be greatly improved (>90%).

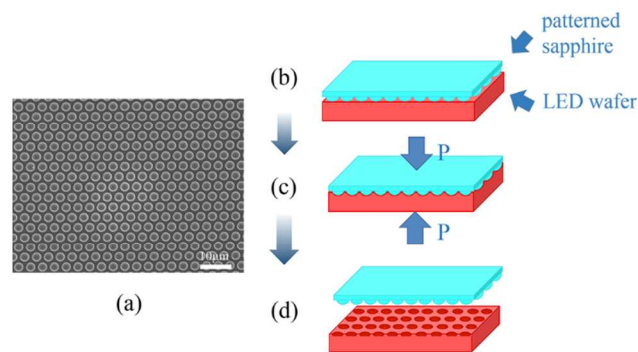


Fig. 1. (a) Top view SEM image of the patterned sapphire. (b-d) Schematic illustration of the fabrication process to create indentation patterns on AlGaInP LED wafer by using patterned sapphire as arrayed indenters.

## Results and discussion

Indentation technique has a long history that can be traced back to the experiment by Heinrich Hertz who first studied two axis-symmetric objects placed in contact in the 1880s. Currently, indentation techniques are mainly used for examining mechanical behaviours of solids. Their potentials on fabricating nanostructured patterns have not been explored. In this present study, we used patterned sapphire as arrayed indenters to create large area indentation pits on AlGaInP LEDs. As shown in Fig.

2(a), highly uniformed indentation pits with a lattice constant of  $3\ \mu\text{m}$  and a diameter of  $\sim 100\ \text{nm}$  were fabricated. Note that the red background originates from light emitted from the MQWs upon excitation by the light source of the optical microscope. Figure. 2(b) shows a low magnification plane view SEM image of the indentation pits, in which moderate surface damages and microcracks emanated from the indents can be visualized. Figure. 2(c) shows a high magnification plane view SEM image of an individual indentation pit. The pit is circular in shape with a diameter of  $\sim 450\ \text{nm}$ , and surrounded by ring and radial cracks. The formation of ring cracks is consistent with the Hertzian fracture model, which predicts the initiation of ring cracks at solid surface and propagation downward and outward into a truncated cone configuration.<sup>23</sup> In contrast, the formation of radial cracks is determined by the crystallographic features. In this case, AlGaInP alloys are typical cubic crystals, characterized by a slip system in which slip occurs in  $\langle 110 \rangle$  directions on  $\{111\}$  planes, resulting in cleavages on  $\{110\}$  planes.<sup>24</sup> For the AlGaInP LED wafer used in our experiments, the GaP window layer is oriented in the direction with the (511) crystal plane exposed. For spherical indentation on crystals, previous studies revealed that fractures occur along the cleavage planes due to dislocation pileups.<sup>25</sup> The intersection of  $\{110\}$  planes with (511)-plane lead to the formation of crack path in  $\langle 1\bar{1}6 \rangle$  and  $\langle 11\bar{6} \rangle$  crystallographic directions with an intersection angle of  $105^\circ$ , as revealed in Fig. 2(c).

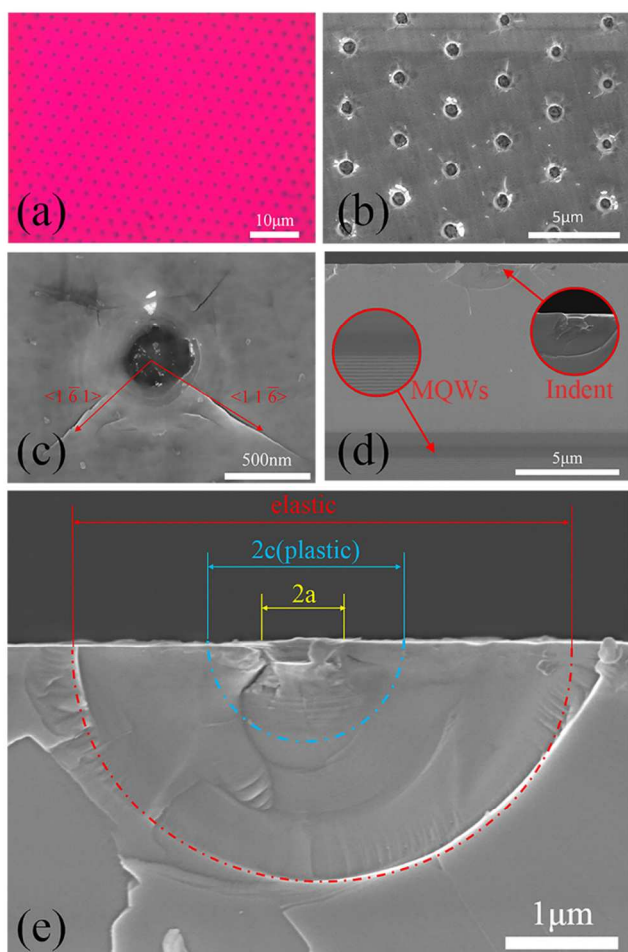


Fig. 2. (a) Optical image of the AlGaInP LED surface after indentation. (b) Low magnification plane view SEM image of the AlGaInP LED after indentation. (c) High magnification plane view SEM image of an individual indentation pit. The

cracks follow the  $\langle 1\bar{6}1 \rangle$  and  $\langle 11\bar{6} \rangle$  crystallographic directions, respectively. (d) Cross sectional SEM image showing the separation between an indentation pit and multiple quantum wells (MQWs). (e) Cross sectional SEM image of an indentation pit with the pit, plastic and elastic regions marked.

Figure 2(d) shows a low magnification cross sectional SEM image of the LED sample. It is evident that the damaged zone induced by indentation are limited in a spherical region, far from the MQWs. The insets of Fig. 2(d) show the high magnification SEM images of an indentation pit and the multiple quantum wells (MQWs), respectively. It is evident that the MQWs remain undamaged. Based on the indentation theory,<sup>23</sup> we estimate the cracks can only reach 1~2  $\mu\text{m}$  below the surface while the thickness of the GaP layer is 8  $\mu\text{m}$ . As a result, one can expect that the electrical properties of the LEDs will change very little.

Figure 2(e) shows a cross sectional SEM image of an individual indentation pit, in which the cone cracks, plastic zone and elastic zone can be clearly visualized. The indentation pit has a penetration depth of  $\sim 100$  nm, surrounded by a plastic

zone with a diameter of  $\sim 1$   $\mu\text{m}$  and an elastic deformed zone with a diameter of  $\sim 2.3$   $\mu\text{m}$ . Note the cone cracks located inside the plastic zone.

Figure 3 shows the IV curves and the dynamic resistance of the original and patterned samples. The threshold voltage of the patterned sample is  $\sim 20$  mV higher than the original one. The dynamic resistance of the patterned sample is higher than the original one before reaching the working voltage where the IV curves coincide. This observation can be attributed to the indentation damage, e.g., cracks and plastic deformations. The voltage of the patterned sample remains slightly greater than the original sample along with increasing the driving current. However, when the driving current reached 20 mA, the difference simply vanished, suggesting that the MQWs stay intact.

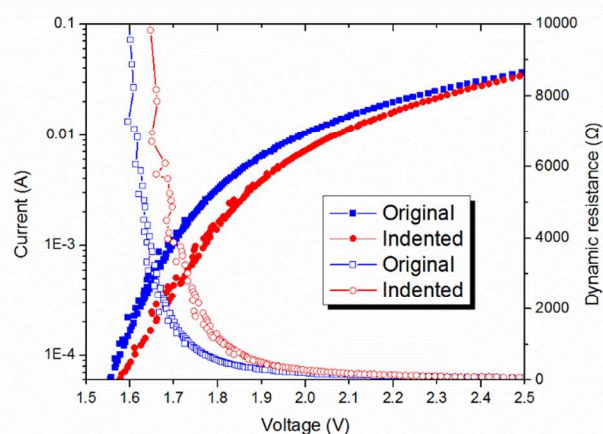


Fig. 3. I-V curves and dynamic resistance of the original and indented chips.

Similar to PCs, one would expect that the indentation pits will alternate the emission profile of planar LEDs. Consequently, we performed angle-resolved electroluminescent (EL) tests for both the original and indented samples at an injection current of 20 mA, as shown in Fig. 4(a). The EL intensities for the indented sample are much greater than the original sample at any angles, with enhancement ratio gradually increasing from 50% at  $15^\circ$  ( $165^\circ$ ) to 70% at  $60^\circ$  ( $120^\circ$ ). The angle-resolved EL spectrum is circular in shape, which differs from the emission profile of photonic crystals, indicating the absence of photonic band gaps. An integration over all angles result in an enhancement ratio of 155%. Figure 4(b) shows the EL spectra of both samples obtained at  $45^\circ$ . The emission peaks are located at 630 nm, without change of peak position and the full width at half maximum (FWHM).

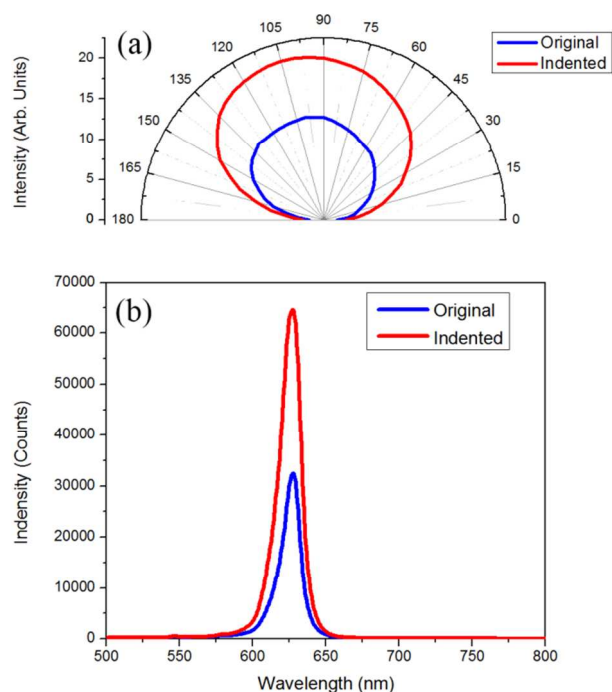


Fig. 4. (a) Angle resolved EL spectra of the original and indented samples. (b) EL spectra of original and indented samples measured at  $45^\circ$ .

We discuss the observations based on optical effects caused by indentation damage, with emphasis on crack and residual strains. It is well known that stress applied to a solid changes its optical properties. For example, an optically isotropic crystal becomes birefringent under the action of an external stress. We can calculate the induced change in the optical indicatrix by  $\Delta B_{ij} = p_{ijkl} S_{kl}$ , where  $p_{ijkl}$  are the components of the photoelastic (strain-optic) tensor and  $S_{kl}$  are the residual strain in the GaP layer. The residual stress fields around indents are usually quite complicated, with values in the range of several hundreds of MPa, as experimentally determined by X-Ray diffraction (XRD).<sup>26</sup> In the case of GaP, the Young's modulus of GaP is 156.2 GPa. The residual stresses can only change the optical index by  $\sim 0.1\%$ . However, we believe that the contribution to disturbing the total refraction may not be ignored in consideration of the high refractive index of GaP. In fact, the residual stress field forms an inhomogeneous strain field characterized by graded refractive index between the surface pattern and the MQWs. The existence of this layer intercepts the guided modes, resulting in increased LEE. It should also be pointed out that the indentation cracks could play a very important role on light extraction. Both the ring and radial cracks may deflect optical waves and create new channels for light extraction.

## Conclusions

In summary, periodic hemispherical pits have been successfully fabricated on AlGaInP LEDs by mechanical indentation using patterned sapphire. It is confirmed that this technique can be

utilized to increase the EL intensity by 155%. The damages induced by indentation are confirmed to have negligible effects on electrical conductivity, but can greatly increase the light extraction efficiency. This method is simple, facile, and quite cost effective. We expect that it can be extended to other optoelectrical devices with improved performance.

## Acknowledgements

The authors thank National Science Foundation of China (NSFC) (Grant No. 91123007, 91233122, 51472143), the Innovation Projects of Shandong University (Grant No. 2014JC031 and 2014YQ003), and National Basic Research Program of China (973 Program) (Grant No. 2009CB930503) for financial support.

## Notes and references

<sup>a</sup> State Key Laboratory of Crystal Materials, Shandong University, 27 South Shanda Road, Jinan, Shandong 250100, P. R. China.

- 1 E. F. Schubert, in *Light Emitting Diodes*. (Cambridge University Press, Cambridge, 2006).
- 2 D. S. Wu, W. K. Wang, W. C. Shih, R. H. Horng, C. E. Lee, W. Y. Lin, and J. S. Fang, *IEEE Photon. Technol. Lett.*, 2005, **17**, 288.
- 3 F. M. Steranka, in *Semiconductors and Semimetals*. (Academic, San Diego, 1997).
- 4 Th. Gessmann, *J. Appl. Phys.*, 2004, **95**, 2203.
- 5 M. R. Krames, O. B. Shchekin, R. M. Mach, G. O. Mueller, L. Zhou, G. Harbers, and M. G. Craford, *J. Disp. Technol.*, 2007, **3**, 160.
- 6 G. Lin, Z. Zuo, D. Liu, Z. Feng, Q. Zhang, X. Lin, and X. Xu, *J. Phys. Chem. C*, 2013, **117**, 27062.
- 7 F. Urbach, *Phys. Rev.*, 1953, **92**, 1324.
- 8 Y. C. Lee, S. H. Tu, and B. Cui, in *Recent Advances in Nanofabrication Techniques and Applications* (InTech, Rijeka, 2011) p.173.
- 9 K. Okamoto, I. Niki, A. Shvartser, G. Maltezos, Y. Narukawa, T. Mukai, Y. Kawakami, and A. Scherer, *Phys. Status Solidi A*, 2007, **204**, 2103.
- 10 C. Huh, K. Lee, E. J. Kang, and S. J. Park, *J. Appl. Phys.*, 2003, **93**, 9383.
- 11 C. E. Lee, Y. C. Lee, H. C. Kuo, T. C. Lu, and S. C. Wang, *IEEE Photonics Technol. Lett.*, 2008, **20**, 803.
- 12 T. Fujii, Y. Gao, R. Sharma, E. L. Hu, S. P. DenBaars, and S. Nakamura, *Appl. Phys. Lett.*, 2004, **84**, 855.
- 13 H. Y. Ryu, J. K. Hwang, Y. J. Lee, and Y. H. Lee, *IEEE J. Sel. Top. Quant. Electron.*, 2002, **8**, 231.
- 14 H. Wang, S. Zhou, Z. Lin, T. Qiao, L. Zhong, K. Wang, X. Hong and G. Li, *RSC Adv*, 2014, **4**, 41942
- 15 C. Y. Cho, S. J. Lee, J. H. Song, S. H. Song, S. H. Hong, S. M. Lee, Y. H. Cho, and S. J. Park, *Appl. Phys. Lett.*, 2011, **98**, 051106.
- 16 W. C. Peng, Y. Chung, and S. Wu, *Appl. Phys. Lett.*, 2006 **89**, 041116.
- 17 T. Kim, P. O. Leisher, A. J. Danner, R. Wirth, K. Streubel, and K. D. Choquette, *IEEE Photonics Technol. Lett.*, 2006, **18**, 1876.

- 18 M. L. Hsieh, K. C. Lo, Y. S. Lan, S. Y. Yang, C. H. Lin, H. M. Liu, and H. C. Kuo, *IEEE Photonics Technol. Lett.*, 2008, **20**, 141.
- 19 Y. Zhao, F. Yan, H. Gao, Y. Zhang, et al. Photonics Asia 2007. International Society for Optics and Photonics, Beijing, China, 12–14 November 2007, edited by J. Li, Y. Fan et al.(SPIE, Bellingham, 2007), pp. 684103-684103.
- 20 R. W. Dixon, *J. Appl. Phys.*, 1967, **38**, 5149.
- 21 C. Hardy, C. N. Baronet, and G. V. Tordion, *Int. J. Numer. Meth. Eng.*, 1971, **3**, 451.
- 22 F. Cripps and A. C. in *Introduction to Contact Mechanics*. (Springer, New York, 2007).
- 23 B. R. Lawn and T. R. Wilshaw, in *Fracture of brittle solids*. (Cambridge university press, Cambridge 1975).
- 24 J. E. Ayers, in *Heteroepitaxy of semiconductors: theory, growth, and Characterization*. (CRC press, 2007).
- 25 D. Liu, M. Chelf and K. W. White, *Acta Metall.*, 2006, **54**, 4525.
- 26 M. Leoni, P. Scardi, and V. M. Sglavo, *J. Euro. Ceram. Soc.*, 1998, **18**, 1663.

### Table of contents entry

Periodic indentation patterns fabricated on AlGaInP light emitting diodes (LEDs) and the schematic diagrams of the indentation process as inserted.

